 doi:10.20944/preprints202112.0064.v1

Article

Lanthanum oxide obtention from different spent fluid catalytic cracking catalysts

Lorena Alcaraz[1,2], Olga Rodríguez Largo[1], Francisco J. Alguacil[1], Margarita Álvarez Montes[3], Carmen Baudín[2], and Félix A. López[1,*]

[1] Centro Nacional de Investigaciones Metalúrgicas (CENIM-CSIC), Avda. Gregorio del Amo 8, 28040, Madrid, Spain; alcaraz@cenim.csic.es, olga.rodriguez@csic.es, fjalgua@cenim.csic.es, f.lopez@csic.es
[2] Instituto de Cerámica y Vidrio, (ICV-CSIC), Kelsen 5, 28049, Madrid, Spain; cbaudin@icv.csic.es
[3] Refractarios Alfran, Pol. Ind. Hacienda Dolores, 41500, Alcalá de Guadaíra, Sevilla, Spain; mam@alfran.com

* Correspondence: f.lopez@csic.es

Abstract: An laboratory-scale procedure has been developed to obtain lanthanum oxide from spent fluid catalytic cracking catalyst, commonly used in the cracking the heavy crude oil process. Two different spent fluid catalytic cracking catalysts, which are mainly formed by silica and alumina, and a certain amount of rare earths were leached under several conditions to recover the rare earth from the solids waste. Subsequently, liquid phases were subjected to a liquid-liquid extraction process, and lanthanum was quantitatively stripped using oxalic acid to obtain the corresponding lanthanum oxalates. After the corresponding thermal treatment, these solids were transformed into lanthanum oxide. Both, lanthanum oxalates and oxides solids have been characterized by wide techniques in order to investigate the purity of the phases.

Keywords: spent fluid catalytic cracking catalyst; waste slag; leaching; lanthanum oxide; rare earths recovery

1. Introduction

Fluid catalytic cracking catalyst (FCC catalyst) is a widely process used in crude oil processing in petroleum refineries, which consists to crack the heavy crude oil into lighter products under the action of catalyst at high temperature [1,2]. The FCC catalyst process was established in the last century in order to improve gasoline production and increase the octane number of the fuel [3]. However, this process consumes a great amount of catalyst. It is estimated that more than 700,000 tons are consumed worldwide annually [4]. Normally, FCC catalyst consists of a rare earth-ultra-stabilized zeolite (USY-zeolite) held in an amorphous silica-alumina matrix [5,6]. The use of rare earths (REEs) in FCC catalysts, especially La and Ce, arose from the need for the use of more active and stable products, with a high yield performance [7,8]. REEs addition improves the catalytic activity and prevents the loss of acid sites during operation [7].

During the process, the FCC catalyst is frequently purged and replaced with a fresh catalyst to manage the process performance [9]. The withdrawn material discharged during the FCC catalyst process is called spent FCC catalyst (sFCC), or equilibrium catalyst (Ecat). This waste slag contains amounts of different elements such as REEs and aluminum [2,10] among others. The amount of spent FCCs generated annually is uncertain or even unknown. Nevertheless, some estimations in recent years have estimated production of 840,000 tonnes per year [8] reveals the great extension of the problem. Most of the spent FCC are disposed of in landfills [11], which leads to serious environmental pollution and human health problems so it is must be treated properly. Because of sFCC consists mainly of active silica (SiO_2) and alumina (Al_2O_3), the final spent FCC catalyst can subsequently be employed as cement raw material, or as a partial replacement of cement or sand in cement mortars [12,13]. However, the amount of spent catalyst that can be incorporated

 doi:10.20944/preprints202112.0064.v1

in cementitious materials is limited and the added value of such kind of applications is low. Due to the relatively high amounts of alumina and silica in spent FCC catalysts, an attractive option for decreasing the environmental impact generated by their final disposal is their recycling as feedstock of mullite refractories. Such an application would admit large volumes of material to be recycled and spare large volumes of minerals [14].

On the other hand, due to their unique physicochemical properties, REEs are indispensable elements in the high technology industry and are widely used in a variety of advanced applications [2,4,15]. Due to the key roles in the lifestyle, and their wide variety of uses in electrical and electronic technology development, the demand for rare earths increases day-to-day indicating that natural resources requirements will also continue to increase [16]. Secondary resources such as manufacturing waste and used rare-earth-based materials could be an interesting alternative for REEs demand even and that secondary-resource processing will become a necessity [17].

Rare earth oxide widely used in catalysts is lanthanum oxide (La_2O_3). Thus, considering the great amount of spent FCC generated and its content of REEs, recovery of La from the recycling of spent FCC materials could be an important source of this rare earth [18].

Hydrometallurgical methods which involve leaching, precipitation, solvent extraction, and/or ion exchange processes have been reported to metal recovery from different waste [19,20].

REEs recovery from spent FCC has previously been reported using different conditions such as mineral acids [21], basic media [22], and/or organic acids [23]. Even different leaching conditions to extract REEs from the sFCC solid have been reported [19,21]. However, despite that numerous laboratory-scale studies have been published regarding the recovery of REEs from several residues or waste [21], no processes were developed on an industrial scale.

In this work, an laboratory-scale process for lanthanum extraction from two spent FCC catalysts with very different amounts of La_2O_3, and the final obtention of La_2O_3 was assessed. In subsequent work, the evaluation of the insoluble residues obtained from the process as raw materials for refractories is reported. In this sense, the final amounts of impurities, in particular of La_2O_3, and the alumina/silica ratio in the insoluble residues will be analyzed for its application [14].

Several conditions were analyzed to recovery lanthanum from the spent fluid catalytic cracking catalyst initial solids by a leaching process. Different leaching agents, as well as concentrations, were evaluated. Subsequently, liquid-liquid extraction was carried out to selectively separate the rare-earth of interest. Various conditions were also assessed. Finally, lanthanum stripped in the liquid phase was precipitated, and the solid formed was thermally treated to obtain pure lanthanum oxide as products.

2. Materials and Methods

The two different spent fluid catalytic cracking powders were investigated, named as SC1 and SC2.

2.1. Leaching process of the spent fluid catalytic cracking powders

Different conditions were evaluated in order to recover lanthanum from the spent fluid catalytic cracking powders (FCC) (SC1 and SC2). Hydrochloric acid (HCl), nitric acid (HNO_3), oxalic acid ($C_2H_2O_4$, OA), and sodium hydroxide (NaOH) were used.

SC1 SC2 were put in contact with a leaching solution into a glass reactor at 60 °C for 4 hours at a 100 g/L pulp density. The leaching process was carried out into a great-capacity glass reactor. Previous investigations have been reported that the leaching efficiencies of the metals increase with the temperature [2]. The final mixtures were filtered, and the final solids were dried. Lanthanum content in each liquid phase was analyzed to evaluate the efficiency of the process.

Preprints (www.preprints.org) | NOT PEER-REVIEWED | Posted: 6 December 2021 doi:10.20944/preprints202112.0064.v1

2.2. Liquid-liquid extraction procedure

Aqueous feed solutions from the highest lanthanum recovery were used for the extraction experiments. For the liquid-liquid extraction experiments, the extractant used in the present investigation is the commercially available Cyanex 923, which is composed of four phosphine oxides (R_3PO, $R_2R'PO$, $RR_2'PO$, and R_3PO) where R = n-octyl and R' = n-hexyl. The extractant was used undiluted or diluted in Solvesso 100 (aromatic diluent).

Extractions are carried out in thermostatic separator funnels provided of mechanical shaking via a four blades impeller (2.5 cm diameter). Various aqueous to organic (A/O) ratios were investigated. After phases disengagement typically 2-3 minutes, lanthanum and acid content remaining in the raffinate (aqueous solution) were analysed. Their content in the equilibrated organic phases was calculated by the mass balance.

Lanthanum content in liquid phases was analyzed by Inductively Coupled Plasma Optical Emission Spectrometry (ICP-OES). In addition, acid content was analyzed by titration with standard NaOH solution using bromothymol blue as indicator.

2.3. Stripping

The stripping step was carried out with oxalic acid using the organic extracted solution under the optimal conditions. These experiments were performed with 1 M oxalic acid solution as stripping phase according to the next equation:

$$\mathrm{L}\cdot \mathrm{La(NO)}_{3,org} + 3\mathrm{C_2O_{4,org}^{2-}} \Leftrightarrow \mathrm{L_{org}} + \mathrm{La_2(La_2O_4)_3} + 3\mathrm{NO_{3,aq}^{-}} \qquad (1)$$

The precipitates were then centrifuged, and subsequently calcinated at 1200 °C for 2 hours in order to yield the La_2O_3 phase.

It should be noted that in the described process the extractant is regenerated, thus, it can be recycled and reused to another extraction step.

2.4. Characterization

The chemical composition of the starting powders was determined by X-ray fluorescence (XRF) using a PANalytical Axios wavelength-dispersive spectrometer (4kW).

Lanthanum content in the liquid phases was analyzed by Inductively Coupled Plasma-Optical Emission Spectrometry (ICP-OES) using an Agilent 5100 VDV model, with an associated analytical error of ±2%.

The structural characterization of the final solids was carried out by X-ray diffraction (XRD) using a Siemens D5000 diffractometer equipped with a Cu anode (Cu $K_{\alpha 1}$ radiation) and a LiF monochromator.

Thermal decomposition of the precursor powders was analyzed by thermogravimetric analysis (TGA) and differential thermal analysis (DTA) using a differential thermal analyzer from 20 °C to 900 °C with a 10 °C/min heating rate, using as an inert medium helium gas, and aluminum oxide was used as reference material.

Fourier-transformed infrared spectroscopy (FTIR) using a Varian 670 FTIR spectrometer within the frequency range 4000-400 cm^{-1} in transmittance mode with a spectral resolution of 4 cm^{-1} was also performed. Measurements were carried out using the KBr pellet technique.

Finally, the morphological characterization was realized by scanning electron microscopy (SEM) using a JEOL-6400 electron microscope operating at 20 kV. For sample preparation, the powder samples were placed on an adhesive conductive carbon disk and gold-coated.

3. Results and discussion

The chemical compositions of the two starting spent FCC catalyst powders obtained by XRF are shown in Table 1. According to the bibliography [7], both powders are mainly composed by alumina and silica. The nature and amounts of minor impurities are similar while the La_2O_3 contents are significantly different.

Preprints (www.preprints.org) | NOT PEER-REVIEWED | Posted: 6 December 2021 doi:10.20944/preprints202112.0064.v1

Table 1. Chemical composition (wt %) for both spent FCC powders.

Oxide (wt %)	SC1	SC2
Al_2O_3	50.00	52.20
SiO_2	45.60	39.10
La_2O_3	1.82	4.32
V_2O_5	nd	0.24
Na_2O	0.19	0.30
P_2O_5	0.94	0.27
TiO_2	0.89	0.64
Fe_2O_3	0.43	0.36
CeO_2	nd	0.26
NiO	0.12	nd
MgO	nd	0.88
SO_3	nd	1.25

3.1. Leaching of the spent FCCs

Different leaching tests in order to recover lanthanum from both powders were carried out using a leaching agent concentration of 2 M. Tables 2 and 3 show lanthanum recovery percentages from both starting powders, modifying the leaching agent.

Table 2. Experimental conditions and lanthanum recovery of the different tests carried out from SC1 powder.

Experiment	Leaching agent	La recovery (%)
Nº 1	HCl	81
Nº 2	HNO_3	82
Nº 3	OA	11
Nº 4	NaOH	26

Table 3. Experimental conditions and lanthanum recovery of the different tests carried out from SC2 powder.

Experiment	Leaching agent	La recovery (%)
Nº 5	HCl	84
Nº 6	HNO_3	85
Nº 7	OA	32
Nº 8	NaOH	10

As can be appreciated, lanthanum recovery from both starting powders using OA as well as NaOH was poor. Therefore, these experimental conditions were discarded. The highest extraction percentages of both REE were obtained when HCl and HNO_3 were used as leaching agents.

In order to increase the lanthanum recovery percentage, several additional tests were carried out using HNO_3 in the same experimental conditions (i.e. 60 ºC for 4 hours, at a 100 g/L pulp density), but varying the leaching agent concentration. The obtained results are summarized in Table 4.

Preprints (www.preprints.org) | NOT PEER-REVIEWED | Posted: 6 December 2021 doi:10.20944/preprints202112.0064.v1

Table 4. Experimental conditions and lanthanum recovery of the different tests carried out from both starting powders.

HNO_3 (M)	SC1		SC2	
	Nº	La recovery (%)	Nº	La recovery (%)
2	2	82	6	85
1.5	9	97	12	95
1	10	47	13	74
0.5	11	66	14	83

The obtained results showed that the highest recovery percentage was found using a leached concentration of 1.5 M. Table 5 shows the chemical composition obtained by XRF for both insoluble residue powders (called SC1-B and SC2-B, respectively) after the leaching treatment under optimal conditions. Lanthanum content in the final solids was practically despicable. As can also be appreciated in Table 5, lanthanum extraction from the spent fluid catalytic cracking catalysts leads to partial extraction of aluminum from the solids.

Table 5. Chemical composition (wt %) for both spent FCC insoluble residue powders.

Oxide (wt %)	SC1-B	SC2-B
Al_2O_3	38.6	44.5
SiO_2	59.2	52.7
La_2O_3	0.33	0.52
V_2O_5	nd	0.15
Na_2O	nd	nd
P_2O_5	0.25	0.096
TiO_2	1.12	0.87
Fe_2O_3	0.26	0.23
CeO_2	nd	0.28
NiO	0.15	<0.05
MgO	nd	0.47
SO_3	nd	0.18
Al_2O_3/SiO_2	0.65	0.84

It should be noted that, according to the obtained results from leaching experiments, liquid phases obtained by nitric acid of 1.5 M (i.e. Nº 9 and Nº 12) were selected due to their higher lanthanum content.

3.2. Extraction of the REE from the spent FCC

After the as-described acid leaching for both starting spent FCC powders, the recovery of lanthanum from the corresponding liquid phases was investigated using liquid-liquid extraction methodology. Starting liquid solutions are composed by 1.1 g/L La and 1.5 M nitric acid.

3.2.1. Extraction of lanthanum from leaching solutions

Preprints (www.preprints.org) | NOT PEER-REVIEWED | Posted: 6 December 2021 doi:10.20944/preprints202112.0064.v1

Previous experiments showed that the equilibrium of both lanthanum and nitric acid extractions reached after 5 min of contact between the organic phase and acid aqueous feed solutions. Thus, 10 min were used as contact time through all experimentation.

The effect of the aqueous/organic ratio (A/O ratio), and the extractant concentration on lanthanum and nitric acid loading onto the organic phase were investigated. The results of these investigations were shown in Figure 1 and Figure 2 for lanthanum and nitric acid extractions, respectively.

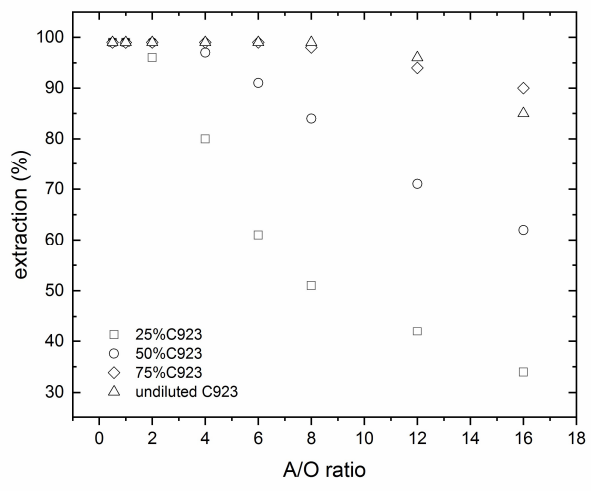

Figure 1. Lanthanum extraction at various Cyanex 923 concentrations. Temperature: 20 °C.

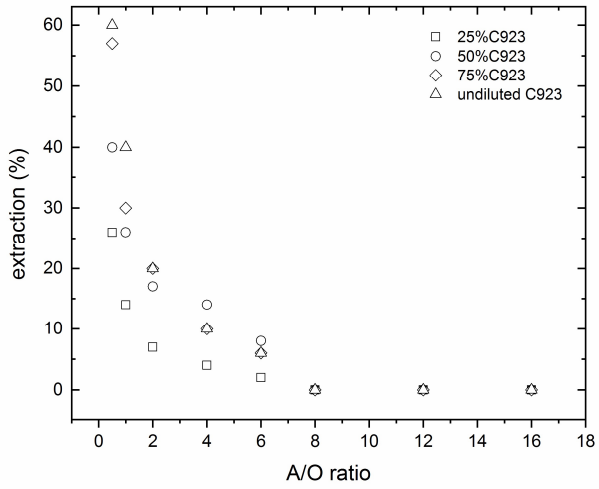

Figure 2. Nitric acid extraction at various Cyanex 923 concentrations. Temperature: 20 °C.

In the case of lanthanum, the percentage of lanthanum extraction increased with the extractant concentration (i.e. A/O low ratios), where lanthanum was practically quantitatively extracted from the leach solution.

The responsible equilibrium for the lanthanum extraction could be represented by the Equation 2:

$$La^{3+}_{aq} + 3NO^{-}_{3,aq} + L_{org} \Leftrightarrow L \cdot La(NO_3)_{3,org} \qquad (2)$$

where L is the organic extractant, and the subscripts *aq* and *org* are the aqueous and organic phases, respectively.

Preprints (www.preprints.org) | NOT PEER-REVIEWED | Posted: 6 December 2021 doi:10.20944/preprints202112.0064.v1

The extraction constant for the above equilibrium (Equation 3) can be defined as:

$$k_{ext} = \frac{[La(NO_3)_3 \cdot nL]_{org}}{[La^{3+}]_{aq} \cdot [NO_3^-]^3_{aq} \cdot [L]^n_{org}} \qquad (3)$$

and considering the definition of the lanthanum distribution coefficient (Equation 4):

$$D_{La} = \frac{[La^3]_{org}}{[La^3]_{aq}} \qquad (4)$$

where $[La^{3+}]_{org}$ and $[La^{3+}]_{aq}$ are the total metal concentrations in the organic and aqueous phases at equilibrium, respectively.

Thus, by substituting in (Equation 2) and the subsequent rearranging leads to the Equation 5:

$$\log D_{La} = C + n \cdot \log [L]_{org} \qquad (5)$$

A plot of $\log D_{La}$ versus $\log [L]_{La}$, for the experimental data obtained in the present work, allowed to estimate the value of the stoichiometric n coefficient. Such plot, indicated that the slope had the value of 3.4 ($r^2 = 0.9636$), thus it was logical to attribute the value of 3 for the n coefficient in Equation 3.

Once the above estimation was done, the experimental data were treated numerically by a tailored computer program in order to confirm the proposed model. This program searched the best set of extraction constants that minimized the squares error sum, defined as:

$$U = \Sigma(\log D_{exp} - \log D_{calc})^2 \qquad (6)$$

where D_{exp} and D_{calc} are the experimental and calculated metal distribution coefficients, respectively. D_{calc} was obtained by solving the mass balance equation for lanthanum, extractant and nitrate, assuming a set of species and constants.

The best fit was obtained using the formation of $La(NO_3)_3 \cdot 3L$ species in the organic phase, as derived from the graphical treatment of the data, with a value of the extraction constant according to:

$$\log k_{ext} = -1.10MAX - 0.88, \text{ and } U = 0.113 \qquad (7)$$

In the case of the nitric acid extraction (Figure 2), similar results were found. The nitric acid extraction decreases with the A/O ratio. Despite that, at the lowest A/O ratio investigated (i.e. A/O=0.5), the maximum nitric acid extraction reached 60% when undiluted Cyanex 923 was used as extractant phase.

The obtained results evidenced that the separation of lanthanum from the nitric acid might have been plotted as Figure 3.

Preprints (www.preprints.org) | NOT PEER-REVIEWED | Posted: 6 December 2021 doi:10.20944/preprints202112.0064.v1

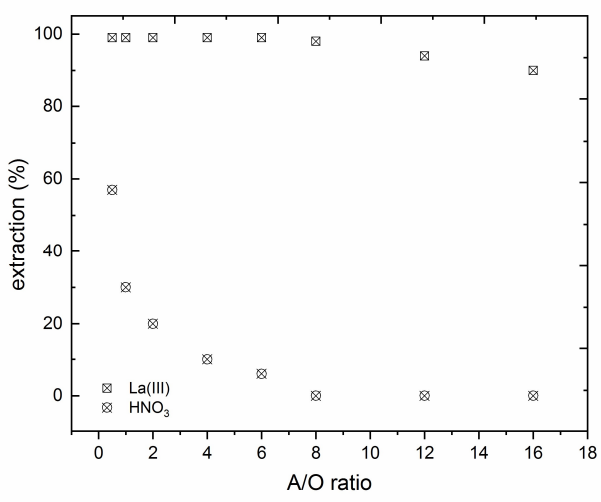

Figure 3. Separation La(III)-HNO_3 at various A/O ratios. Organic phase: 75% v/v Cyanex 923 in Solvesso 100. Temperature: 20 °C.

Effectively, using the and A/O ratio of 8, a quantitative La-HNO_3 was yielded, since D_{La}=355, and not nitric acid extraction was achieved. In this condition, lanthanum concentration in the organic phase reached 7.8 g/L, thus a metal concentration factor near 8 was reached just in one step (it should be noted that the initial concentration of lanthanum in the aqueous phase was 1.1 g/L). Moreover, after the proper acid adjustment, the raffinate can be recycled to another leaching step.

The responsible equilibrium for the nitric acid extraction could be represented by Equation 8 at these nitric acid concentrations (at around 1-2 M), since the value of the extraction constant was dependent on the diluent used in the organic phase [24].

$$H^{+}_{aq} + NO^{-}_{3,aq} + L_{org} \Leftrightarrow 3HNO_{3,org} \qquad (8)$$

3.4. Characterization of the final solid products

3.4.1. X-ray diffraction (XRD)

XRD patterns of the final solids are shown in Figure 4. In the case of the stripped solids using oxalic acid Figure 4a, not well-defined diffraction maxima were obtained. These results could be due to the possible presence of the organic phase in the powder samples. After the stripping with the organic phase, an insignificant amount of Cyanex 923 could adhere onto the surface of the particles, resulting in an amorphous diffraction pattern. Despite this, the diffraction maxima can be attributed to the lanthanum oxalate in both cases. These results reveal the formation of the lanthanum oxalate phase as a unique phase, which can be used as a precursor to the corresponding rare earth oxides.

After the subsequent thermal treatment at 1200 °C for 2 hours of both samples, several diffraction maxima were found in the XRD patterns Figure 4b. All diffraction maxima can be indexed to a La_2O_3 phase. Miller index for the more intense diffraction maxima are also shown in each corresponding peak. No peaks attributable to secondary phases were detected within the sensitivity of the experimental system used, which reveals the purity of the obtained samples. These results reveal that it is possible to recover lanthanum from spent FCC catalysts and to reach a yield lanthanum oxide.

Preprints (www.preprints.org) | NOT PEER-REVIEWED | Posted: 6 December 2021 doi:10.20944/preprints202112.0064.v1

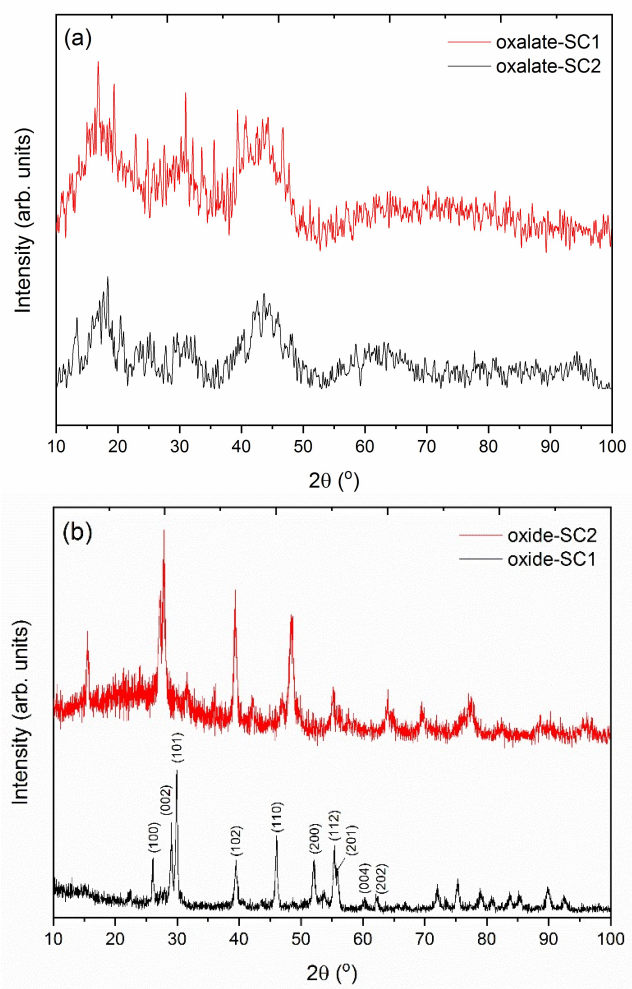

Figure 4. XRD patterns of (a) the stripped precursor solids and (b) after the subsequent thermal treatment.

3.4.2. Thermogravimetric analysis (TGA) and differential thermal analysis (DTA)

Thermal decomposition of the stripping solids was examined by thermogravimetric analysis (TGA) and differential thermal analysis (DTA). Similar thermal decomposition behaviour was found in both precursor samples. As an example, Figure 5 exhibits DTA/TGA curves for the lanthanum oxalate sample obtained after the corresponding stripping step.

Different endothermic peaks were found. First, an endothermic peak can be observed between the range of 106 °C-191 °C with a maximum centered at 135 °C with a mass loss of about 5.9 wt%, which can be assigned to the loss of two water molecules to the lanthanum oxalate decahydrate. On the other hand, a second endothermic peak can be appreciated between 191°C - 385°C (T_{max} = 249 °C) corresponding to a mass loss of 23.3 wt%. This result could be attributed to the loss of six water molecules and the lanthanum oxalate anhydre formation. The next endothermic peak appears between the range of 383 °C - 488 °C (T_{max} = 424 °C) with a mass loss of 21 wt% can be assigned to the formation of lanthanum carbonate basic or La-dioxycarbonate, according to Equation 8:

$$La_2(C_2O_4)_3 \rightarrow La_2O_2CO_3 + 3CO + 2CO_2 \qquad (8)$$

Preprints (www.preprints.org) | NOT PEER-REVIEWED | Posted: 6 December 2021 doi:10.20944/preprints202112.0064.v1

Finally, the last endothermic peak can be observed at around 745 °C - 840 °C (T_{max} = 800 °C), which corresponds to the lanthanum oxide formation with a mass loss of about 4.9 wt%, according to the Equation 9:

$$La_2O_2CO_3 \rightarrow La_2O_3 + CO_2 \qquad (9)$$

The thermal decomposition of lanthanum oxalate decahydrate has previously been described by Grivel et al. [25] and Purwani et al. [26] through three steps: first, the loss of 10 water molecules to form the acetate anhydre; next, the formation of lanthanum carbonate basic, and finally, the formation of lanthanum oxide. In this sense, lanthanum oxalate decomposition has been reported by Balboul et al. [27] according to twelve steps, which also include the loss of water molecules, the formation of different basic carbonates ($La_2(CO_3)_2$, $La_2O(CO_3)_2$ y $La_2O_2CO_3$) and finally, the formation of lanthanum oxide. Zhan et al. [28] described the decomposition of lanthanum oxalate decahydrate through three endothermic dehydration reactions in which the loss of six, two, and two water molecules occurs followed by the formation of lanthanum carbonate basic (T_{max} = 410 °C), and the formation of lanthanum oxide (T_{max} = 708 °C).

The dehydration process proposed in the present work is slightly different in the dehydration stages. This result could be a consequence of the obtention process of the lanthanum oxalate by precipitation with oxalic acid in an organic medium.

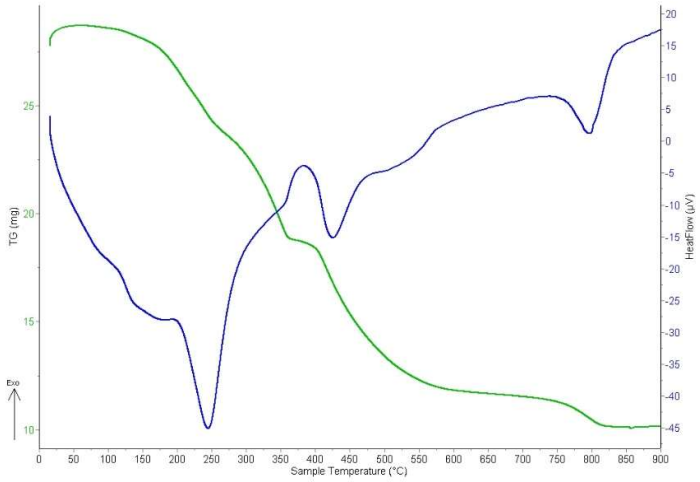

Figure 5. DTA/TGA curves of the obtained lanthanum oxalates.

3.4.3. Fourier Transform Infrared (FTIR)

FTIR spectra of lanthanum oxalates are exhibited in Figure 6. The corresponding assignations of each registered band are also shown in it [29–31]. It can be appreciated a broad emission band peaked at 3500 cm^{-1} that can be attributed to the –OH of the carboxylic group. According to their structure, oxalates do not exhibit this type of H^+ so that the presence of this band suggested the presence of the coordinate H_2O molecules, and a strong link between the chemical structure and the oxalate. Other bands at around 1600 cm^{-1} and 1500 cm^{-1}, which can be attributed to the asymmetric and the symmetric vibrations of the carboxylate group, respectively, can also be appreciated. The intense band at around 1300 cm^{-1} corresponds to the asymmetric tension of the C-O bond. A typical band of this type of compound was found at 800 cm^{-1}, and corresponds to the vibration of the La-O bond, as well as the bending of the O-C=O group. In addition, a band at around 650 cm^{-1} was registered related to the water molecules content. Finally, the band at 500 cm^{-1} is related to the La-O bond vibration, and the chelated ligand ring deformation.

Preprints (www.preprints.org) | NOT PEER-REVIEWED | Posted: 6 December 2021 doi:10.20944/preprints202112.0064.v1

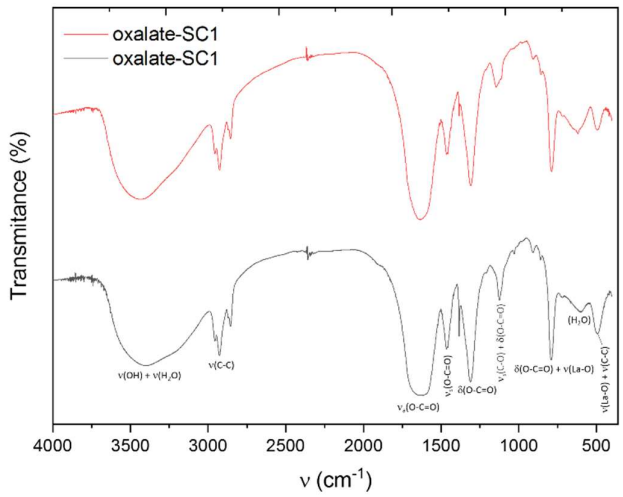

Figure 6. FTIR spectrum of the obtained oxalates.

3.4.4. Scanning electron microscopy (SEM)

Figure 7 exhibits SEM micrographs of the lanthanum oxalates (Figure 7a,b) obtained from both initial sFCC powders, and the corresponding lanthanum oxides after the thermal treatment (Figure 7c,d).

Particles agglomerates with approximately sheet-like particles were found in the case of the obtained lanthanum oxalates (Figure 7a,b). After the thermal treatment at 1200 °C for 2 hours (Figure 7c,d), the powder samples exhibit nanoparticles agglomerates with an irregular particle shape and size. This morphology is in good agreement with that previously reported in calcined samples of La_2O_3 composition [32].

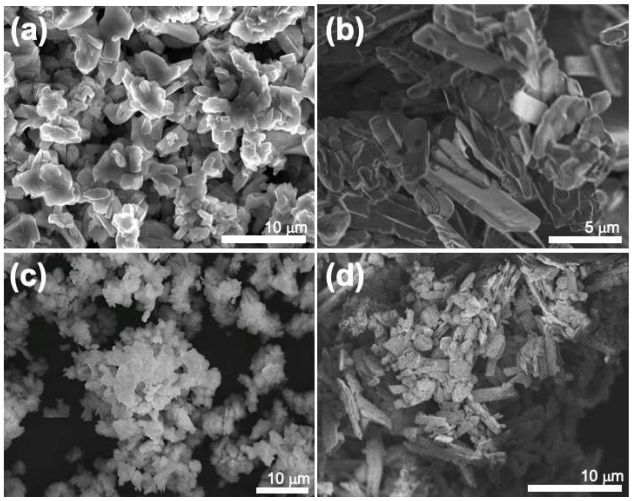

Figure 7. SEM micrographs of (a-b) lanthanum oxalates and (c-d) lanthanum oxides samples.

5. Conclusions

An effective process to obtain lanthanum oxide from spent fluid catalytic cracking (sFCC) catalysts has been assessed. Two different sFCC solids were used in the investigated work. First, acid leaching was evaluated under different conditions to extract lanthanum from the initial solids. Leaching using nitric acid with a 1.5 M concentration proved to be the most effective condition for the recovery of lanthanum for both samples investigated.

 doi:10.20944/preprints202112.0064.v1

Subsequently, liquid-liquid extraction process was investigated to selectively separate lanthanum from nitric acid. Optimal separation was found for A/O ratio of 8. Finally, lanthanum was stripped from the organic phases using oxalic acid to precipitate the corresponding lanthanum oxalate. After a thermal treatment, lanthanum oxide was effectively obtained. The present work demonstrate that it is possible to obtain lanthanum oxide from spent fluid catalytic cracking catalysts by the as-described industrial-scale procedure.

Author Contributions: L.A. methodology, validation, formal analysis, investigation, writing—original draft preparation, writing; O.R.L., F.J.A., M.A.M., C.B., and F.A.L. methodology, validation, formal analysis, investigation; F.J.A, C.B. and F.A.L., conceptualization, methodology investigation, writing—review and editing, funding acquisition, supervision, project administration. All authors have read and agreed to the published version of the manuscript.

Acknowledgments: Thanks to CEPSA Research Center (Spain).

Conflicts of Interest: The authors declare no conflict of interest.

References

1. Le, T.; Wang, Q.; Ravindra, A. V.; Li, X.; Ju, S. Microwave intensified synthesis of Zeolite-Y from spent FCC catalyst after acid

activation. *J. Alloys Compd.* **2019**, *776*, 437–446, doi:10.1016/j.jallcom.2018.10.316.

2. Wang, J.; Huang, X.; Cui, D.; Wang, L.; Feng, Z.; Hu, B.; Long, Z.; Zhao, N. Recovery of rare earths and aluminum from FCC waste slag by acid leaching and selective precipitation. *J. Rare Earths* **2017**, *35*, 1141–1148, doi:10.1016/j.jre.2017.05.011.
3. Sposato, C.; Catizzone, E.; Blasi, A.; Forte, M.; Romanelli, A.; Morgana, M.; Braccio, G.; Giordano, G.; Migliori, M. Towards the circular economy of rare earth elements: Lanthanum leaching from spent FCC catalyst by acids. *Processes* **2021**, *9*, 1–15, doi:10.3390/pr9081369.
4. Zhou, Y.; Schulz, S.; Lindoy, L.F.; Du, H.; Zheng, S.; Wenzel, M.; Weigand, J.J. Separation and recovery of rare earths by in situ selective electrochemical oxidation and extraction from spent fluid catalytic cracking (FCC) catalysts. *Hydrometallurgy* **2020**, *194*, 105300, doi:10.1016/j.hydromet.2020.105300.
5. Silva, J.S.; Medeiros de Jesus-Neto, R.; Fiuza, R.A.; Gonçalves, J.P.; Mascarenhas, A.J.S.; Andrade, H.M.C. Alkali-activation of spent fluid cracking catalysts for CO_2 capture. *Microporous Mesoporous Mater.* **2016**, *232*, 1–12, doi:10.1016/j.micromeso.2016.06.005.
6. Senter, C.; Mastry, M.C.; Zhang, C.C.; Maximuck, W.J.; Gladysz, J.A.; Yilmaz, B. Role of chlorides in reactivation of contaminant nickel on fluid catalytic cracking (FCC) catalysts. *Appl. Catal. A Gen.* **2021**, *611*, 117978, doi:10.1016/j.apcata.2020.117978.
7. Akah, A. Application of rare earths in fluid catalytic cracking: A review. *J. Rare Earths* **2017**, *35*, 941–956, doi:10.1016/S1002-0721(17)60998-0.
8. Ferella, F.; D'Adamo, I.; Leone, S.; Innocenzi, V.; De Michelis, I.; Vegliò, F. Spent FCC E-Cat: Towards a Circular Approach in the Oil Refining Industry. *Sustainability* **2018**, *11*, 113, doi:10.3390/su11010113.
9. Maidel, M.; Ponte, M.J.J. de S.; Ponte, H. de A.; Valt, R.B.G. Lanthanum recycling from spent FCC catalyst through leaching assisted by electrokinetic remediation: Influence of the process conditions on mass transfer. *Sep. Purif. Technol.* **2022**, *281*, 119905, doi:10.1016/j.seppur.2021.119905.
10. Wang, J.; Huang, X.; Wang, L.; Wang, Q.; Yan, Y.; Zhao, N.; Cui, D.; Feng, Z. Kinetics study on the leaching of rare earth and aluminum from FCC catalyst waste slag using hydrochloric acid. *Hydrometallurgy* **2017**, *171*, 312–319, doi:10.1016/j.hydromet.2017.06.007.
11. Akcil, A.; Vegliò, F.; Ferella, F.; Okudan, M.D.; Tuncuk, A. A review of metal recovery from spent petroleum catalysts and ash. *Waste Manag.* **2015**, *45*, 420–433, doi:10.1016/j.wasman.2015.07.007.
12. Al-Jabri, K.; Baawain, M.; Taha, R.; Al-Kamyani, Z.S.; Al-Shamsi, K.; Ishtieh, A. Potential use of FCC spent catalyst as partial replacement of cement or sand in cement mortars. *Constr. Build. Mater.* **2013**, *39*, 77–81, doi:10.1016/j.conbuildmat.2012.05.035.
13. Vogt, E.T.C.; Weckhuysen, B.M. Fluid catalytic cracking: recent developments on the grand old lady of zeolite catalysis. *Chem. Soc. Rev.* **2015**, *44*, 7342–7370, doi:10.1039/C5CS00376H.
14. Restrepo, E.; Vargas, F.; López, E.; Baudín, C. The potential of La-containing spent catalysts from fluid catalytic cracking as feedstock of mullite based refractories. *J. Eur. Ceram. Soc.* **2020**, *40*, 6162–6170, doi:10.1016/j.jeurceramsoc.2020.04.051.
15. Maheshwaran, G.; Selva Muneeswari, R.; Nivedhitha Bharathi, A.; Krishna Kumar, M.; Sudhahar, S. Eco-friendly synthesis of lanthanum oxide nanoparticles by Eucalyptus globulus leaf extracts for effective biomedical applications. *Mater. Lett.* **2021**, *283*, 128799, doi:10.1016/j.matlet.2020.128799.
16. Balaram, V. Rare earth elements: A review of applications, occurrence, exploration, analysis, recycling, and environmental impact. *Geosci. Front.* **2019**, *10*, 1285–1303, doi:10.1016/j.gsf.2018.12.005.
17. Jyothi, R.K.; Thenepalli, T.; Ahn, J.W.; Parhi, P.K.; Chung, K.W.; Lee, J.-Y. Review of rare earth elements recovery from secondary resources for clean energy technologies: Grand opportunities to create wealth from waste. *J. Clean. Prod.* **2020**, *267*, 122048, doi:10.1016/j.jclepro.2020.122048.
18. Chiranjeevi, T.; Pragya, R.; Gupta, S.; Gokak, D.T.; Bhargava, S. Minimization of Waste Spent Catalyst in Refineries. *Procedia Environ. Sci.* **2016**, *35*, 610–617, doi:10.1016/j.proenv.2016.07.047.

19. Weigand, M.W.S.K.G.M.R.K.N.L.T.T.H.L.A.D.V.S.G.J. *Hydrometallurgical Recovery of Rare Earth Metals from Spent FCC Catalysts*; 2016; ISBN 9783319486161.
20. Sadeghi, M.; Jesus, J.; Soares, H. Recycling spent fluid cracking catalysts for rare earth metal recovery: A review. *Reciklaza i Odrziv. Razvoj* **2018**, *11*, 43–52, doi:10.5937/ror1801043M.
21. Zhao, Z.; Qiu, Z.; Yang, J.; Lu, S.; Cao, L.; Zhang, W.; Xu, Y. Recovery of rare earth elements from spent fluid catalytic cracking catalysts using leaching and solvent extraction techniques. *Hydrometallurgy* **2017**, *167*, 183–188, doi:10.1016/j.hydromet.2016.11.013.
22. Wang, J.; Xu, Y.; Wang, L.; Zhao, L.; Wang, Q.; Cui, D.; Long, Z.; Huang, X. Recovery of rare earths and aluminum from FCC catalysts manufacturing slag by stepwise leaching and selective precipitation. *J. Environ. Chem. Eng.* **2017**, *5*, 3711–3718, doi:10.1016/j.jece.2017.07.018.
23. Lin, X.; Fan, Y.; Liu, Z.; Shi, G.; Liu, H.; Bao, X. A novel method for enhancing on-stream stability of fluid catalytic cracking (FCC) gasoline hydro-upgrading catalyst: Post-treatment of HZSM-5 zeolite by combined steaming and citric acid leaching. *Catal. Today* **2007**, *125*, 185–191, doi:10.1016/j.cattod.2007.02.023.
24. Alguacil, F.J.; López, F.A. The extraction of mineral acids by the phosphine oxide Cyanex 923. *Hydrometallurgy* **1996**, *42*, 245–255, doi:10.1016/0304-386X(95)00101-L.
25. Grivel, J.-C.; Zhao, Y.; Suarez Guevara, M.J.; Watenphul, A. Studies on the thermal decomposition of lanthanum(III) valerate and lanthanum(III) caproate in argon. *Thermochim. Acta* **2015**, *612*, 1–9, doi:10.1016/j.tca.2015.05.002.
26. Purwani, M. V; Suyanti, S.; Adi, W.A. Thermal composition kinetics of lanthanum oxalate hydrate product treatment from monazite. *J. Sains Mater. Indones.* **2019**, *20*, 50, doi:10.17146/jsmi.2019.20.2.5295.
27. A.A. Balboul, B.; El-Roudi, A.M.; Samir, E.; Othman, A.G. Non-isothermal studies of the decomposition course of lanthanum oxalate decahydrate. *Thermochim. Acta* **2002**, *387*, 109–114, doi:10.1016/S0040-6031(01)00834-6.
28. Zhang, G.; Yu, J.; Xu, Z.; Zhou, F.; Chi, R. Kinetics of thermal decomposition of lanthanum oxalate hydrate. *Trans. Nonferrous Met. Soc. China* **2012**, *22*, 925–934, doi:10.1016/S1003-6326(11)61266-1.
29. Dumitru, R.; Negrea, S.; Ianculescu, A.; Păcurariu, C.; Vasile, B.; Surdu, A.; Manea, F. Lanthanum Ferrite Ceramic Powders: Synthesis, Characterization and Electrochemical Detection Application. *Materials (Basel).* **2020**, *13*, 2061, doi:10.3390/ma13092061.
30. Bîrzescu, M.; Niculescu, M.; Dumitru, R.; Carp, O.; Segal, E. Synthesis, structural characterization and thermal analysis of the cobalt(II) oxalate obtained through the reaction of 1,2-ethanediol with $Co(NO_3)_2 \cdot 6H_2O$. *J. Therm. Anal. Calorim.* **2009**, *96*, 979–986, doi:10.1007/s10973-009-0054-z.
31. Nakamoto, K. *Infrared and Raman Spectra of Inorganic and Coordination Compounds*; John Wiley & Sons, Inc.: Hoboken, NJ, USA, 2008; ISBN 9780470405840.
32. Karthikeyan, S.; Selvapandiyan, M. Effect of annealing temperature on the properties of lanthanum oxide (La_2O_3) nanoplates by reflux routes. *Int. J. Eng. Sci. Res. Technol.* **2018**, *7*, 559–562, doi:10.5281/zenodo.1202124.